



WILEY
Blackwell

the FEBS Journal

Volume 280 Number 6 March 2013 | ISSN 1742-464X

www.febsjournal.org



Review Article
Hsp90 as a drug target for cancer



Depletion of Aurora-A in zebrafish causes growth retardation due to mitotic delay and p53-dependent cell death

Hee-Yeon Jeon and Hyunsook Lee

Department of Biological Sciences and Institute of Molecular Biology and Genetics, Seoul National University, Korea

Keywords

apoptosis; Aurora-A; p53; spindle assembly checkpoint; zebrafish

Correspondence

H. Lee, Department of Biological Sciences and Institute of Molecular Biology and Genetics, Seoul National University, Daehak-dong, Gwanak-gu, Seoul 151-742, Korea.

Fax: +82 2 886 4335

Tel: +82 2 880 9121

E-mail: HL212@snu.ac.kr

Website: <http://biosci.snu.ac.kr/hyunlee>

(Received 5 November 2012, revised 16 January 2013, accepted 22 January 2013)

doi:10.1111/febs.12153

Aurora-A is a serine/threonine mitotic kinase that is required for centrosome maturation. Many cancer cells over-express Aurora-A, and several reports have suggested that Aurora-A has prognostic value in the clinical treatment of cancer. Therefore, inhibitors for Aurora-A kinase have been developed. However, studies on Aurora-A are largely performed in cancer cell lines and are sometimes controversial. For effective evaluation of Aurora-A inhibitors in cancer treatment, it is essential to understand its function at the organism level. Here, we report the crucial functions of Aurora-A in homeostasis of spindle organization in mitosis using zebrafish embryogenesis as a model system. Using morpholino technology, we show that depletion of Aurora-A in zebrafish embryogenesis results in short bent trunks, accompanied by growth retardation and eventual cell death. Live-imaging and immunofluorescence analyses of the embryos revealed that the developmental defects are due to problems in mitosis, manifested through monopolar and disorganized spindle formation. Aurora-A-depleted cells exhibited mitotic arrest with congression failure, leading to activation of the spindle assembly checkpoint. Cell death in the absence of Aurora-A was partially rescued by co-injection of the p53 morpholino, suggesting that apoptosis after Aurora-A depletion is p53-dependent. The clinical implications of these results relate to the indication that Aurora-A inhibitors may be effective towards cancers with intact p53.

Introduction

Cell division culminates with mitosis, where segregation of the duplicated genome occurs. Mitosis is orchestrated by kinases: CDK1/cyclin B is the master kinase and regulates mitosis, followed and synergized by the activities of mitotic kinases such as Aurora-A, Aurora-B and polo-like kinase 1 (Plk1). These kinases have distinct functions and also work in concert to regulate mitosis.

The first *aurora* allele was identified in a screen for *Drosophila* mutants that displayed defective spindle-

pole behavior. When the *Aurora* gene is mutated, microtubule spindles radiate from the single pole and the chromosomes form a rosette-like structure, implying that the *aurora* allele is involved in the regulation of centrosomes and the assembly of proximal spindles [1]. Other studies have shown that *Drosophila* has two Aurora kinases, while mammals have three Aurora kinases (Aurora-A/B/C) with a conserved serine/threonine kinase domain [2]. Whereas Aurora-B kinase localizes to the centromeres and regulates

Abbreviations

MO, morpholino; SAC, spindle assembly checkpoint; TUNEL, terminal deoxynucleotidyl transferase dUTP nick end labeling; zfAurora-A, zebrafish Aurora-A.

bi-orientation of chromosomes, Aurora-A kinase has been reported to be crucial in centrosome maturation [3]. Some reports have suggested that Aurora-A is also implicated in the regulation of mitotic entry in circumstances such as serum starvation and checkpoint recovery [4,5].

Human Aurora-A, located at chromosome 20q13.2, is commonly amplified in numerous malignant tumors, including breast, colon, bladder, ovary, skin and pancreatic cancers, and the levels of Aurora-A mRNA and protein are increased in many tumors [6–8]. Therefore, inhibition of Aurora-A kinase is an attractive target for the treatment of cancer [9]. However, controversial results have been obtained regarding the function of Aurora-A. Cell line studies indicated that *Aurora-A* is an oncogene [10], whereas studies on *Aurora-A* knockout mice showed that the haploinsufficient Aurora-A mouse developed tumors and suggested that Aurora-A may be a tumor suppressor [11].

Furthermore, clinical efforts to inhibit Aurora-A activity in the treatment of cancer revealed that the situation is more complicated than first thought. In some clinical trials, Aurora kinase inhibitors showed disappointing results [12]. This may be due to off-target effects on other Aurora family kinases. As inhibition of Aurora-B kinase over-rides the mitotic checkpoint activation [13], inhibition of both Aurora-A and Aurora-B may give complicated results. Another possibility is that evaluation of the Aurora-A inhibitors was first performed in cell lines, where genes that genetically interact with Aurora-A have been mutated. Therefore, investigations on Aurora-A at the organism level are required.

We propose that the use of zebrafish (*Danio rerio*) for such studies is beneficial in many ways. The function of Aurora kinase in development has not been fully established due to its early embryonic lethality in mice [11]. In comparison, morpholino-induced knockdown of gene expression in zebrafish embryogenesis is very efficient and does not interfere with maternal transcripts, and thus early embryonic lethality may be avoided. Furthermore, zebrafish eggs are laid *ex utero* and are transparent, enabling monitoring of cell proliferation and the physiological consequences of gene knockdown at the organism level. Another advantage of zebrafish embryogenesis is that there is no limitation of the embryos for manipulation.

Here, we show that zebrafish Aurora-A (zfAurora-A) is crucial in integrity of the organization of the microtubule spindle and establishment of the bipolar spindle assembly in mitosis. Knockdown of *zfAurora-A* led to activation of the spindle assembly checkpoint (SAC) and growth arrest. Moreover, cells lacking

zfAurora-A exhibited apoptosis post-mitosis in a p53-dependent manner. These results confirm the role of Aurora-A in centrosome homeostasis. Furthermore, this work implies that Aurora-A-specific inhibitors may be effective on p53-positive cancers, as opposed to cancers with a p53 mutation.

Results

Zebrafish Aurora-A is critically required for embryonic proliferation during development

We found a putative Aurora-A in zebrafish (zgc:100912; <http://zfin.org>) by searching for human Aurora-A orthologs using bioinformatic tools. Initially, it was designated as serine/threonine protein kinase 6 with unknown function, and is located on chromosome 6 of zebrafish [14]. When we aligned the sequence with human Aurora-A using UniProt (www.uniprot.org), there was 56% similarity in amino acid sequences. The kinase domain (amino acids 138–388 in zfAurora-A) was well conserved, showing 94% similarity with human Aurora-A (Fig. 1A). The amino acid similarity of Aurora-A between *Caenorhabditis elegans*, *Drosophila melanogaster*, *Mus musculus*, *Homo sapiens* and *Danio rerio* (zebrafish) was ~ 33.3%.

To assess the expression level and pattern of *zfAurora-A* expression during the developmental process, RT-PCR and *in situ* hybridization assays were performed. *zfAurora-A* was expressed maternally and zygotically, as the mRNA was detected from four-cell stage embryos (Fig. 1B). *In situ* hybridization revealed that *Aurora-A* was expressed in all proliferating cells until the bud stage. From the 18-somite stage to the prim-6 stage, expression was abundant in the brain, tail, eye, spinal cord and somites, where cellular expansion takes place during these embryonic stages (Fig. 1C). Both maternal and zygotic *Aurora-A* mRNA was ubiquitously expressed in actively dividing cells.

Knockdown of Aurora-A expression leads to growth retardation and cell death

To analyze the function of Aurora-A in zebrafish, we utilized knockdown gene expression using morpholino oligos, and validated the physiological outcome of the loss of function. Morpholinos that block translation of *Aurora-A* (ATG MOs), or splicing morpholinos, targeting the splice junction of exon 4/intron 4, respectively, were injected into embryos at the 1–4-cell stage. Because the results for both Aurora-A morpholinos were similar, we present here the results from the translation-blocking morpholinos (Aurora-A MO).

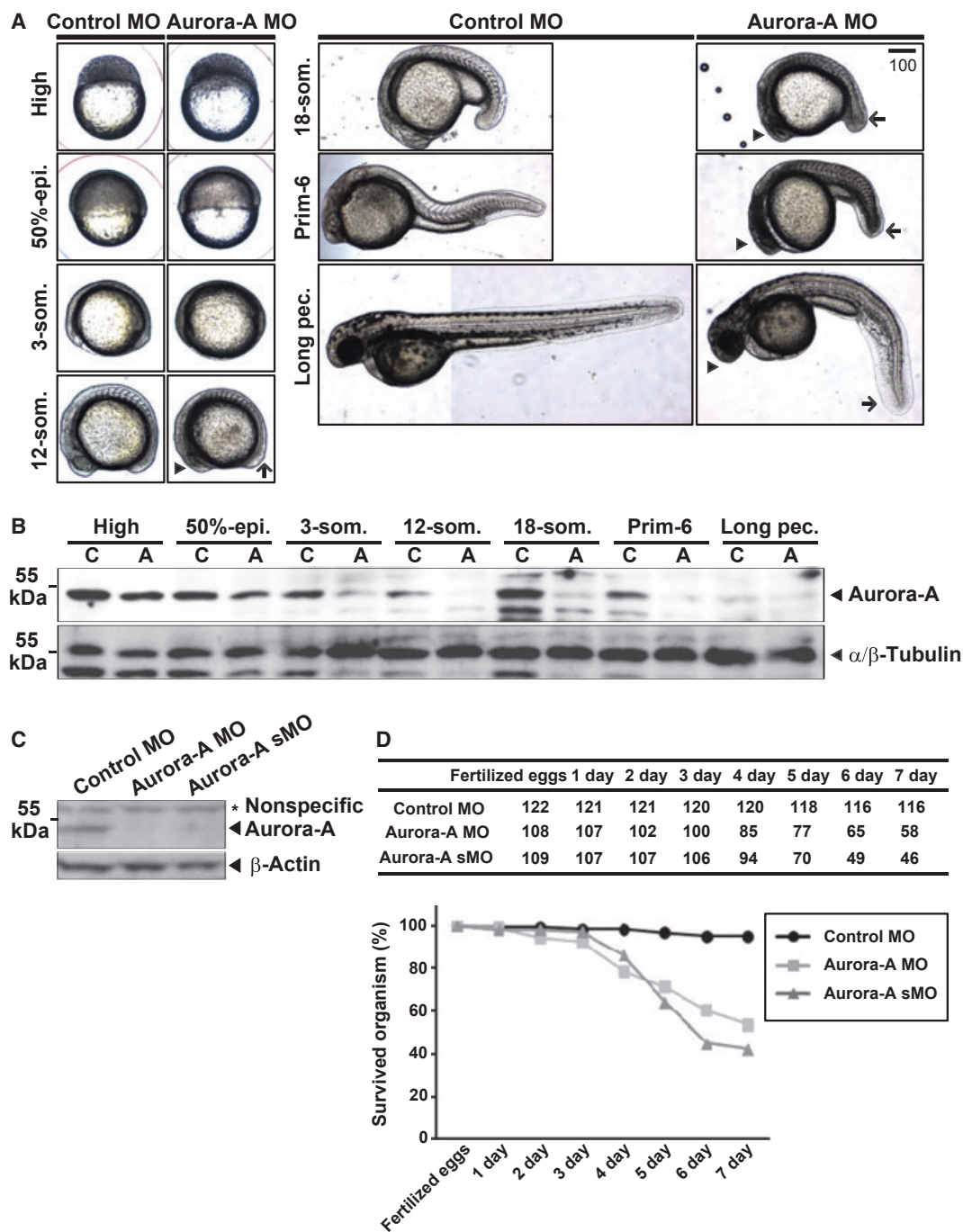


Fig. 2. zfaurora-A morphants display growth defects and cell death. (A) Comparison of control and zfaurora-A morphants from 4-cell stage embryos to the long pectoral fin stage. Arrows and arrowheads indicate apparent growth defects. Images of live embryos immobilized on 3% methylcellulose were obtained using an Axio Imager A1 microscope with a 4 × objective. Scale bar = 100 μm. (B) Determination of the efficiency of knockdown expression by zfaurora-A MO injection using western blotting. The mouse serum against zfaurora-A detects a band of ~ 50 kDa. zfaurora-A disappears upon MO injection from the 3-somite stage, indicating that morpholino injection does not abolish maternal proteins. Extracts from four embryos were loaded per lane. Time post fertilization: High, 3.3 h post-fertilization (hpf); 50% epi., 5.3 hpf; 3-som., 11 hpf; 12-som., 15 hpf; 18-som., 18 hpf; Prim-6, 25 hpf; Long pec., 48 hpf. (C) Western analysis of embryos injected with control MO, Aurora-A MO (ATG MO) and Aurora-A sMO (splicing MO). Analysis was performed at 1 days post-fertilization using four embryos. (D) Viability of embryos injected with control MO, Aurora-A MO (ATG MO) and Aurora-A sMO (splicing MO). The number of live embryos was counted every day. The viability of the injected embryos is shown as a survival graph.

Fig. 3. Knockdown of *zfAurora-A* interferes with mitotic progression. (A) Immunostaining with anti-phospho-histone H3 antibody in the control, *zfAurora-A* morphant, and embryos co-injected with *zfAurora-A* MO and EGFP-*Aurora-A* RNA. pH3-positive cells appear red, and DNA was counter-stained using DAPI (4',6'-diamidino-2-phenylindole). Images were taken using an Axio Observer Z1 microscope with a 20 × objective. Scale bar = 50 μm. (B) Flow cytometric analysis after MPM-2 immunostaining and staining with 7-amino-actinomycin D (7-AAD). 2C and 4C DNA contents measured by 7-AAD staining are shown. The MPM-2-positive 4C DNA contents shown in the rectangular boxes represent cells arrested in mitosis. (C) Immunofluorescence assay with antibodies against α -tubulin and γ -tubulin in fixed embryos at 25 hpf after control or *zfAurora-A* MO injection. Representative prometaphase and metaphase cells are shown in each group. α -tubulin is shown in red, γ -tubulin is shown in green and DNA is shown in blue (counter-stained with DAPI). (D) Co-injection of EGFP-*Aurora-A* with control or *Aurora-A* MO. Expression of EGFP-*Aurora-A* shows that it is localized at centrosomes with γ -tubulin. Images were acquired, processed and deconvoluted using a DeltaVision microscope with a 100 × objective and the SoftWorx program (Applied Precision). Scale bar = 5 μm.

arrows). In 18-somite embryos, the brains of *zfAurora-A* morphants were markedly smaller and morphologically malformed, potentially due to cell death (Fig. 2A, arrowheads). At the prim-6 stage, 25 h post-fertilization (hpf), somite lengthening and yolk extensions were impaired: the width of the somites was reduced, but the number of somites was intact. At 48 hpf (long pectoral stage), *Aurora-A* morphants displayed a markedly smaller brain and eyes, as well as a short bent trunk (Fig. 2A). Western blot analysis using an antibody raised against *zfAurora-A* indicated that *Aurora-A* was successfully depleted from the 3-somite stage (Fig. 2B). Both the ATG MO and the splicing MO similarly depleted *zfAurora-A* (Fig. 2C), suggesting that injection of the splicing MO resulted in knockdown of the protein rather than blocking the splicing. This result supports the notion that the outcomes of injection of ATG MO and the splicing MO were similar. Morpholinos are relatively less effective towards the abundant maternal RNA [15,16]. Therefore, it is not surprising that *Aurora-A* expression is not reduced until the 50% epiboly stage. When overall survival was measured, *Aurora-A* morphants (resulting from injection of either the *Aurora-A* MO or the splicing MO) exhibited death from 4 days post-fertilization, with only 40% of embryos surviving at 6 days post-fertilization (Fig. 2D).

Knockdown of *Aurora-A* expression causes problems in progression through mitosis

Targeted disruption of the *Aurora-A* allele in mice results in embryonic lethality before E7.5 (embryonic day 7) [4]. The fact that injection of *Aurora-A* MOs did not deplete maternal *Aurora-A* indicated to us that morpholino-mediated knockdown of *Aurora-A* may enable us to track and analyze the function of *Aurora-A* in zebrafish during development.

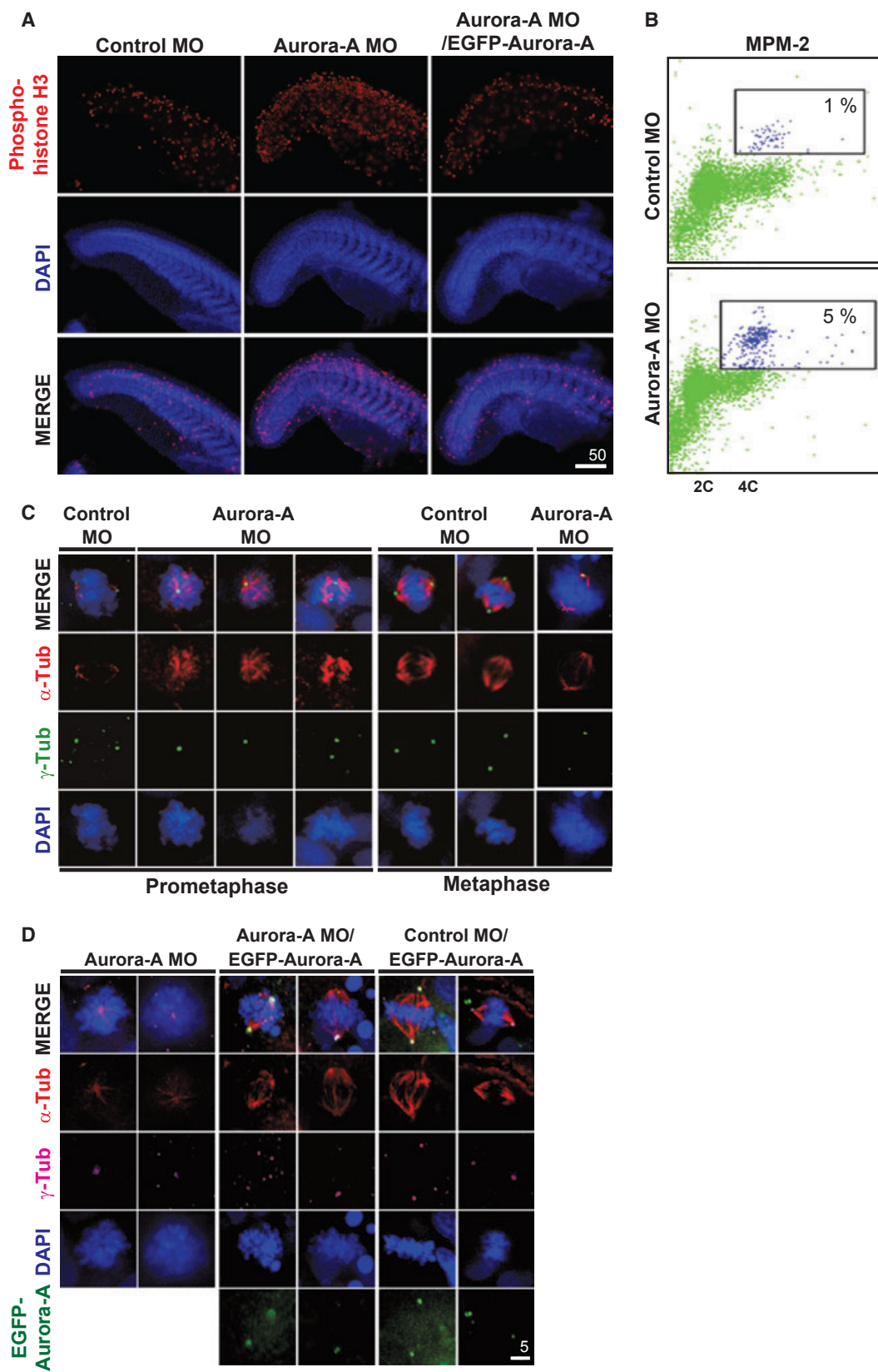
In zebrafish, the advantage is that these mitotic problems may be monitored during embryogenesis outside the uterus over a markedly short period. When

any defects are observed, the embryos may be fixed at that stage for analysis.

To investigate the underlying mechanism of growth retardation, we first determined whether *Aurora-A* depletion resulted in mitotic arrest. Embryos at 25 hpf were fixed and immunostained with antibody against phospho-histone H3 (pH3), which marks late G₂ and early mitosis [17]. *Aurora-A* morphant embryos exhibited a marked increase in pH3-positive cells compared with controls (Fig. 3A, middle column). A positive result for pH3 may indicate that the cells have a high proliferation index or that the cells remain in mitosis. Because the morphant embryos exhibit growth retardation, it is more likely that the *Aurora-A* morphant cells are arrested in mitosis. When GFP-tagged *Aurora-A* RNA was co-injected with the *Aurora-A* MO (Fig. 3A, right column), the pH3 level dropped to a level comparable to the control, indicating that *Aurora-A* depletion leads to mitotic arrest.

To confirm the mitotic arrest, embryos were subjected to immunostaining with an MPM-2 monoclonal antibody, which detects phospho-epitopes in mitosis [18], coupled with 7-amino-actinomycin D (7-AAD) staining to indicate DNA content. Measurement of MPM-2 immunostaining is a useful index to assess SAC activation and mitotic arrest [19,20]. Flow cytometric analysis revealed that *Aurora-A* morphant cells were indeed arrested in mitosis, as the number of MPM-2-positive cells with 4C DNA content increased (Fig. 3B). Collectively, these results suggest that depletion of *zfAurora-A* in zebrafish embryos leads to activation of the SAC and mitotic arrest.

To analyze the basis of SAC activation and mitotic arrest after *zfAurora-A* depletion, embryos were collected at the prim-6 stage, co-immunostained using the antibodies against α -tubulin and γ -tubulin, and subjected to immunofluorescence analysis. In mitosis, 67.4% of *zfAurora-A* morphant cells exhibited abnormal spindle organization ($n = 62$, Fig. 3C): 47.8% ($n = 44$) exhibited monopolar spindles (Fig. 3C, prometaphase, *Aurora-A* MO, 1st and 2nd columns), and



19.6% ($n = 18$) displayed disorganized spindles with two centrosomes (Fig. 3C, prometaphase, Aurora-A MO, 3rd column). Cells with two centrosomes were present in the Aurora-A morphant, but the γ -tubulin immunofluorescence intensity was lower compared to control (Fig. 3C, metaphase, and Fig. S1). In the controls, only 5.7% of mitotic cells (three of 52 cells) displayed abnormal spindles. When *EGFP-zfAurora-A* RNA was injected together with Aurora-A MO, it partially rescued the defect that bipolar cells increased. EGFP-Aurora-A co-localized with γ -tubulin, indicating that zfAurora-A mainly localizes to the centrosomes (Fig. 3D). Together, these results suggest that zfAurora-A is required for the intactness of the centrosome required to establish bipolar spindle assembly.

Aurora-A morphants exhibit delays in mitosis and SAC activation

To assess the consequences of the centrosome abnormality, monopolar spindles and disorganized spindle assembly in embryonic proliferation, a whole-embryo live-imaging technique was used. Histone (H2B)-GFP-expressing transgenic zebrafish embryos [21] were injected with either control or Aurora-A MO to facilitate tracking of chromosome movements, and subjected to time-lapse video microscopy (Fig. 4A–D). Mitotic duration from the nuclear envelope breakdown to anaphase onset was measured in control and Aurora-A morphant, and mitosis was monitored in > 90 cells in at least three embryos. When compared to control (Fig. 4A and Movie S1), zfAurora-A depletion led to congression failure: cells displayed problems aligning the chromosomes and forming the metaphase plate for equal chromosome segregation (Fig. 4B–D and Movies S2–S4). After a long prometaphase arrest, 91.3% of chromosomes ($n = 84$) eventually segregated (Fig. 4B). Some cells (4.4%, $n = 4$) exited mitosis without division, and the chromosomes de-condensed without segregation (Fig. 4C). This exit without segregation has previously been observed in haploinsufficient mouse embryonic fibroblasts (MEFs) of *Aurora-A* knockout mice [4]. Lagging chromosomes were detected in 6.5% of cases ($n = 6$) (Fig. 4D) after chromosome mis-alignment. In two cases (2.2%), cell death within mitosis was detected. With regard to mitotic duration, zfAurora-A morphant cells spent much longer in mitosis: mitotic duration was 15–18 min in controls and ~ 90 min in Aurora-A-depleted cells (Fig. 4E).

Together, these results indicate that zfAurora-A depletion in embryogenesis results in centrosome

abnormality, which then resulted in defects in bipolar spindle establishment that led to activation of the SAC. To corroborate SAC activation, we assessed Mad2 localization at the unattached kinetochore, which reflects initial SAC signaling and activation [22,23]. As a zebrafish Mad2 antibody was not available, we injected *EGFP-zfMad2* mRNA together with the morpholino. Then, 25 hpf embryos were dissociated into single cells to aid immunofluorescence analysis of zfMad2 at the kinetochores. Immunostaining with CREST (human nuclear auto-antibody to centromere) marked the kinetochores. The result showed that zfMad2 localization at the kinetochores increased 4.6-fold after Aurora-A depletion, compared to control cells, confirming that the SAC is activated (Fig. 4F).

Apoptosis in Aurora-A morphant embryos is p53-dependent

In addition to the mitotic arrest, Aurora-A morphants exhibited cell death, which contributed to the growth defects (Fig. 2A). To confirm the apoptosis in Aurora-A morphants, embryos were subjected to a whole-mount *in situ* TUNEL assay after morpholino injection (Fig. 5A). Upon Aurora-A MO injection, TUNEL-positive cells accumulated from the 3-somite stage and beyond. Apoptosis was detected across the whole embryonic body at the 12-somite stage, when primordial development of the head and tail are balanced. At the 18-somite stage, when a distinctive brain and eyes form, apoptosis was apparent in the head region. During the prim-6 stage, when the trunk and tail elongate and yolk extension is apparent, apoptosis was most prominent in the trunk and tail region (Fig. 5A). These results demonstrate that apoptosis takes place in the proliferating zones upon *zfAurora-A* depletion during zebrafish embryogenesis.

For the underlying mechanism of apoptosis after Aurora-A depletion, three pathways may be suggested: post-mitotic apoptosis, apoptosis upon entry into mitosis, and death in mitosis. As the mitotic entry of Aurora-A morphant cells was not hampered in live-imaging analysis (Fig. 4B–D), we ruled out the possibility of apoptosis before mitosis. In addition, as only two of 92 cells exhibited mitotic cell death in the live-imaging analysis, we ruled out this possibility as well. Thus, we determined whether Aurora-A depletion led to post-mitotic apoptosis. We particularly determined whether this process is p53-dependent, because p53 is involved in post-mitotic G₂ arrest [24] or apoptosis [25] in many cases.

To investigate whether p53 is involved in apoptosis upon Aurora-A depletion in zebrafish embryogenesis,

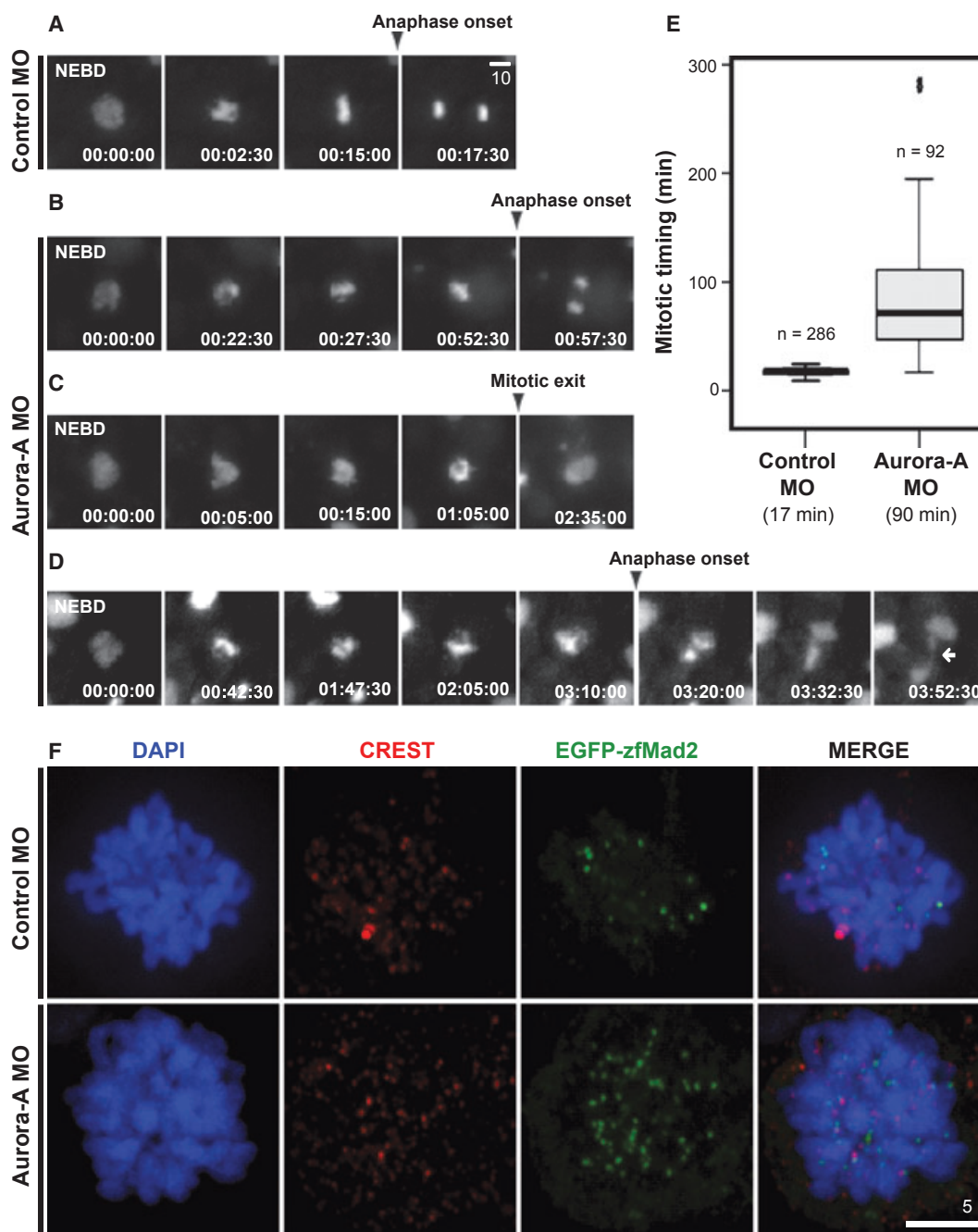


Fig. 4. Delay in mitosis and activation of SAC in zfAurora-A morphant embryos. (A–D) Time-lapse imaging was performed in 25 hpf developing embryos after control or zfAurora-A MO injection. Images were taken of epithelial cells from the yolk surface region. Images were captured every 2.5 min for 7 h. Captured images of representative cells are shown. The time of nuclear envelope breakdown is marked as 0:00. Chromosome segregation and anaphase onset are indicated by arrowheads. Lagging chromosomes are indicated by the white arrow in (D). (E) Mitotic duration for control and zfAurora-A morphants. Control morphants were in mitosis for 15–18 min and zfAurora-A morphants were in mitosis five times longer, for ~90 min. The number of cells analyzed is shown above the bars. The majority of cells exhibited mitotic arrest with congression problems ($n = 84$, 91.3%), while a small number of cells exited from mitosis without division ($n = 4$, 4.35%). Values are means \pm SEM: control, 17 ± 0.08 min; Aurora-A morphants, 90.14 ± 6.58 min. Data were analyzed using SPSS software (SPSS Inc., Chicago, IL, USA). Scale bar = 10 μ m. (F) SAC activation measured by Mad2 localization to the kinetochores. EGFP-zfMad2 was co-injected with morpholinos, embryos were dissociated at 25 hpf, and the cells were immunostained using CREST (red) and anti-GFP (green). Images were taken, processed and deconvoluted using a DeltaVision microscope with a 100 \times objective and the SoftWorx program (Applied Precision). Scale bar = 5 μ m.

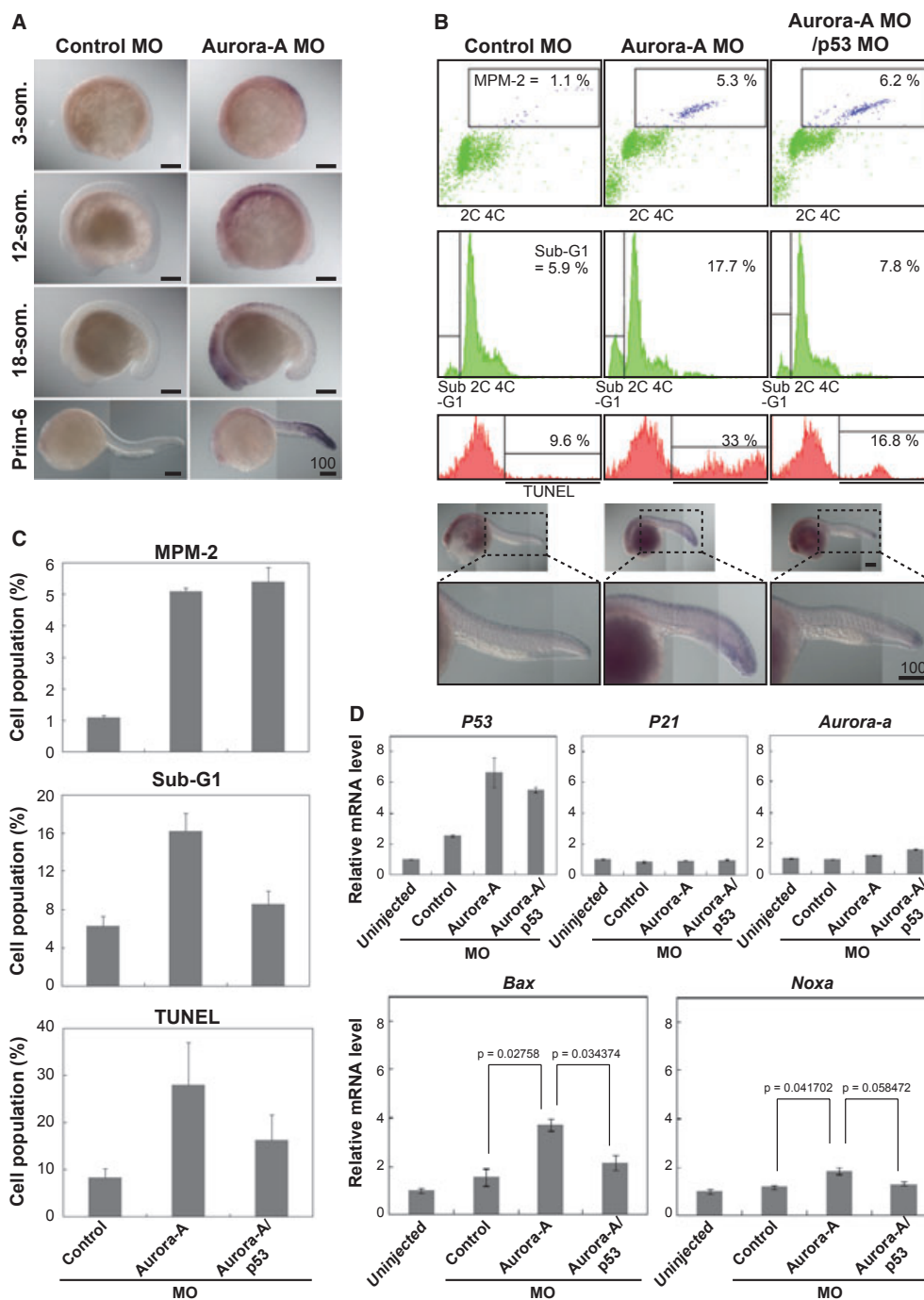


Fig. 5. Apoptosis after zfAurora-A depletion is p53-dependent. (A) Whole-mount *in situ* TUNEL assay to analyze apoptosis in control and zfAurora-A morphants. Scale bar = 100 μ m. (B) Flow cytometry analysis in control, zfAurora-A morphants and zfAurora-A MO and p53 MO double-injected embryos. MPM-2-positive cell populations are marked. The sub-G₁ population (bottom left, middle row) indicated by 7-AAD staining represents apoptotic cells (2nd row). TUNEL-positive cells are indicated by the histograms (3rd row). The numbers indicate the percentage of cells as measured by flow cytometry. This percentage increases markedly in zfAurora-A morphants and is decreased in Aurora-A MO/p53 MO double-injected embryos. The color-labeled TUNEL assay and its enlarged images are shown at the bottom. Images were taken using an Axioplan2 microscope with a 10 \times objective. Scale bar = 100 μ m. (C) Summary of the results of the three independent experiments (Fig. S2) shown in (B) as bar graphs. Values are means + SEM. (D) Quantitative RT-PCR to analyze the mRNA levels in control, zfAurora-A morphants and Aurora-A MO/p53 MO double-injected embryos. Relative expression level of mRNA normalized to β -actin. The results are from three independent experiments. Values are means \pm SEM. *P* values are indicated.

Aurora-A and p53 were simultaneously depleted by injecting Aurora-A MO and p53 MO together. Next, embryos at 25 hpf were dissociated, and single cells were isolated for flow cytometric analysis (Fig. 5B,C and Fig. S2). The sub-G₁ population, indicative of apoptotic cells, increased from 5.9% to 17.7% in the Aurora-A MO-injected group (Fig. 5B, middle panel). This marked increase in the sub-G₁ population was reduced to 7.8% by co-injection of p53 MO (Fig. 5B, middle panel). TUNEL assay after MO injection confirmed that apoptosis in Aurora-A morphants was p53-dependent: TUNEL-positive cells at the tail tip were rescued to a level comparable to control embryos (Fig. 5B, bottom panel). Similarly, apoptosis in the single-cell dissociated-flow cytometric analysis was reduced from 33% to 16.8% when p53 MO was co-injected with Aurora-A MO (Fig. 5B, bottom panel).

Depletion of p53 did not affect mitosis, as the level of MPM-2-positive 4C cells was similar between Aurora-A single morphants and Aurora-A MO/p53 MO double morphants (Fig. 5B, insets in the top panel). Taken together, these results suggest that apoptosis took place after mitosis in a p53-dependent manner.

If apoptosis in Aurora-A morphants is p53-dependent, expression of pro-apoptotic genes that are regulated by p53 should be elevated. To confirm this, 25 hpf embryos were subjected to quantitative real-time RT-PCR analysis after single or double morpholino injection (Fig. 5D). The level of *p53* transcripts increased approximately sevenfold in *zfAurora-A* morphants, indicating that the depletion of Aurora-A induces *p53* expression. This increase in *p53* expression decreased when the p53 MO was co-injected (Fig. 5D, *P53*). However, the decrease was not to a level comparable to that of the control, probably due to the fact that the p53 MO used in this study is the ATG MO, which interferes more with translation than transcription. Concordantly, expression of the p53 downstream target and pro-apoptotic gene *Bax* increased fourfold in the Aurora-A morphant, but this increase decreased to twofold when p53 MO was co-injected (Fig. 5D, *Bax*). *Noxa* transcripts responded similarly to *Bax*; however, the increase was less significant (Fig. 5D, *Noxa*). Compared to the p53-induced pro-apoptotic genes, *Bax* and *Noxa*, the level of expression of the cell-cycle inhibitor gene *p21* was not affected by Aurora-A depletion (Fig. 5C, *P21*), indicating that increase in *p53* expression after Aurora-A MO injection is not the outcome of morpholino cytotoxicity [26] but is specific to the Aurora-A MO injection. Collectively, *zfAurora-A* depletion induces *p53* expression, followed by subsequent activation of *Bax* and *Noxa*, leading to apoptosis.

Discussion

In this study, we showed that Aurora-A is critically required for centrosome intactness and bipolar spindle establishment during zebrafish embryogenesis. Depletion of *zfAurora-A* results in problems in mitotic progression due to the activation of SAC, because SAC is activated upon failure of bipolar spindle attachment [27]. *zfAurora-A*-depleted cells that exited from mitotic arrest underwent apoptosis in the subsequent interphase; this apoptosis was prohibited by blocking p53. Delayed mitosis followed by a certain degree of cell death in Aurora-A morphants resulted in developmental retardation and later death of the embryos. The results shown here indicate that *Aurora-A* is not an oncogene, as had been suggested by reports based on cell culture studies. On the contrary, our studies indicate that the balance of Aurora-A level is crucial in zebrafish embryogenesis. These results have clinical implications, in that application of Aurora-A inhibitors may be effective in cancers with intact *p53*, but not those with mutant *p53*.

The data presented here confirm that the role of Aurora-A kinase in centrosome intactness and spindle formation is evolutionarily conserved. However, we did not detect any defect in mitotic entry upon knockdown of *zfAurora-A*, as had been suggested from cell culture studies. In HeLa cells, antibody injection-mediated Aurora-A depletion induced multipolar spindles and multi-nucleated cells [28], which were not observed in our zebrafish studies. Antibody injection has advantages because one can inhibit the function of the protein at a specific cell cycle stage, by injecting the antibody, without the interference of the results from the previous cell cycle stage. However, the discrepancy with our results may be because HeLa cells usually have inert p53. There is also the antibody epitope issue: antibodies are only able to block the function of the binding site, the N-terminal domain in this case. Therefore, we have confirmed that depletion of Aurora-A function results in monopolar and disorganized spindles. It does not interfere with mitotic exit, which was seen in multi-nucleated HeLa cells after antibody injection. Collectively, zebrafish embryogenesis and morpholino technology provide valuable tools to establish and validate the evolutionarily conserved role of Aurora-A, in addition to defining the roles of Aurora-A *in vivo*.

Cell-cycle regulation is critical in development, as shown in *C. elegans* and *Drosophila* [29]. Previously, we have shown that regulation of mitosis plays a crucial role in embryonic proliferation and therefore is essential in zebrafish embryogenesis [21]. Zebrafish is a valuable cancer model because fish develop tumors

that resemble human tumors [30–32]. The rapid cell division in zebrafish embryogenesis resembles the cell proliferation in tumorigenesis. Because the transparent embryos of zebrafish *ex utero* provide the possibility of monitoring cell proliferation at the organism level, as performed by live imaging, zebrafish embryogenesis offers advantages for deciphering the roles of mitotic players in control of cell proliferation and development. Furthermore, in contrast to cell lines, zebrafish embryos are free from mutations other than the genes being manipulated. Therefore, zebrafish embryos may be useful for *in vivo* drug discovery [33], small molecule screening [34] or drug validation, particularly anti-mitotic kinase inhibitors [21].

Experimental procedures

Fish maintenance

Wild-type zebrafish, *Danio rerio*, were purchased from a local fish store and maintained in appropriate facilities. Eggs were spawned and raised at 28.5 °C, injected with morpholinos or RNAs, and staged according to standard procedures [35].

Cloning of zebrafish *Aurora-A* and *Mad2*

zfAurora-A and *zfMad2* cDNAs were cloned using RT-PCR based on the mRNA sequence in the National Center for Biotechnology Information database (*zfAurora-A*, GenBank accession number NM_001003640.1; *zfMad2*, GenBank accession number NM_001017739). They were first cloned into the pCR-BluntII-TOPO vector (Invitrogen, Carlsbad, CA, USA), and then sub-cloned into the pCS2+EGFP vector [21].

RNA extraction and RT-PCR

Zebrafish embryos were collected at various stages and dechorionated. RNA was extracted using TRIzol (Invitrogen) according to the manufacturer's instructions. Primers for RT-PCR and quantitative RT-PCR were as follows: *zfAurora-A* forward, 5'-CTCCTCCAACACCAGTGGAT-3'; *zfAurora-A* reverse, 5'-GATGCTCCACTCCTGCTTTC-3'; β -actin forward, 5'-CTCTTCCAGCCTTCCTTCCT-3'; β -actin reverse, 5'-CTTCTGCATACGGTCAGCAA-3'; *bax* forward, 5'-ACAGGGATGCTGAAGTGACC-3'; *bax* reverse, 5'-GAAAAGCGCCACAACCTTTC-3'; *noxa* forward, 5'-ATGGCGAAGAAAGAGCAAAC-3'; *noxa* reverse, 5'-CGC TTCCCCTCCATTTGTAT-3'; *tp53* forward, 5'-TTGTCCC ATATGAAGCACCA-3'; *tp53* reverse, 5'-ACACACACGC ACCTCAAAAAG-3'; *p21* forward, 5'-ATGAGGCTCAA ATTGCTGCT-3'; *p21* reverse, 5'-GGCTTTACGTGTGA CCACCT-3'.

In situ hybridization

An antisense RNA probe was synthesized using SP6 RNA polymerase (Roche, Basel, Switzerland) with digoxigenin RNA labeling mix (Roche, Basel, Switzerland), and *in situ* hybridization was performed as described previously [36]. Images were obtained using an Axioplan2 microscope with a 10 × objective and AXIOVISION software (Zeiss, Oberkochen, Germany).

Microinjection of morpholinos (MOs) and sense RNAs

The translation-blocking Aurora-A ATG MO (5'-TGCTTC TTGACCAGAGTCCATATC-3'), the exon 4/intron 4 splicing-blocking Aurora-A MO (5'-ACAGCAGAAGTCC TCCTACCTGAGA-3'), a control MO (5'-CCTCTTACCT CAGTTACAATTTATA-3') and p53 MO (5'-GCGCCATT GCTTTGCAAGAATTG-3') were designed by and purchased from GeneTools (Philomath, OR, USA). Eight nanograms of Aurora-A ATG MO and control MO were injected per embryo, and 4 ng of splicing-blocking Aurora-A MO and p53 MO were injected per embryo. For RNA injection, zebrafish *Aurora-A* and *Mad2* cDNA were sub-cloned into pCS2-EGFP and then transcribed *in vitro* using the mMessage mMachine kit (Ambion, Austin, TX, USA). As EGFP is fused to the N-terminus of Aurora-A, *EGFP-Aurora-A* is not the target of Aurora-A ATG MO. MOs or sense RNA were injected into the yolk of embryos at the 1–4-cell stage.

Antibody generation in mice and western blotting

Antibody for *zfAurora-A* was generated by injecting purified GST-tagged *zfAurora-A* protein into the peritoneum of mice. Mouse serum was diluted with 5% BSA, containing NaCl/Tris/0.1% Tween-20 at 1 : 200 concentration for western blotting. α/β -tubulin antibody (Cell Signaling, Danvers, MA, USA) was used as a loading control. Horseradish peroxidase-conjugated secondary antibodies (Abcam, Cambridge, MA, USA) were used at 1 : 10 000 dilution.

Immunofluorescence assay in whole embryos

Embryos were collected, fixed in 4% paraformaldehyde, and stored in cold methanol. For immunofluorescence preparation, embryos were serially hydrated in NaCl/P_i/0.1% Tween-20, followed by treatment with acetone for 7 min, and then washed twice with NaCl/P_i/0.1% Tween-20. After permeabilization in NaCl/P_i/1% dimethylsulfoxide/0.5% Triton X-100/0.1% Tween₂₀, embryos were incubated with blocking buffer containing 1% BSA and 10% goat serum in NaCl/P_i/0.1% Tween-20. Primary and secondary antibodies were incubated in the blocking solution, washed intensively, and finally mounted using VECTASHIELD Mounting

Medium with DAPI (Vector Laboratories, Burlingame, CA, USA). α -tubulin antibody (Sigma, St Louis, MO, USA), mouse and rabbit γ -tubulin antibody (Sigma), and rabbit phospho-histone H3 (Ser10) antibody (pH3; Millipore, Billerica, MA, USA) were used as primary antibodies, and Alexa Fluor-conjugated secondary antibodies (Invitrogen) were applied. Images of cells at the tip of the tail were taken and processed using an Axio Observer Z1 microscope (Zeiss) or a DeltaVision microscope (Applied Precision, Issaquah, WA, USA). Images acquired using DeltaVision were deconvoluted and processed using the *SOFTWORX* program (Applied Precision).

Flow cytometry

During the prim-6 stage, the embryos were dechorionated, mechanically dissociated into single cells, and fixed with 70% ethanol at -20°C . The cells were then immunostained with MPM-2, followed by staining with 7-amino-actinomycin D (7-AAD) staining before flow cytometric analysis. Apoptotic cells were stained using a fluorescein *in situ* cell death detection kit (Roche). Flow cytometry was performed using a FACSCanto™ II flow cytometer (BD Biosciences, Franklin Lakes, NJ, USA), as described previously [21].

Time-lapse microscopy of live embryos

H2B-GFP transgenic zebrafish [21] were used for live imaging, and epithelial cells from the yolk surface area were recorded. Mitotic duration was measured as the time between nuclear envelope breakdown and anaphase onset/mitotic exit. All procedures were performed as described previously [21].

Analysis of SAC activation by Mad2 localization

In vitro transcribed *EGFP-zfMad2* mRNA was injected with MOs, and then embryos were raised until the prim-6 stage. Embryos were collected and dissociated into single cells, and then centrifuged at 300 *g* for 5 min. Cells fixed with 4% paraformaldehyde were immunostained with CREST (Cortex Biochem, San Leandro, CA, USA) and mounted using Vectashield with 4',6'-diamidino-2-phenylindole. Images were obtained using a DeltaVision microscope, and processed, deconvoluted and analyzed using the *SOFTWORX* program.

TUNEL assay

The whole-mount *in situ* TUNEL assay was performed as described previously [21]. Images were obtained using the same methods as used for the *in situ* hybridization experiments.

Acknowledgements

This work was supported by a National Research Foundation grant funded by the Korean government (2011-0018630 and 2012-0006241), and was also supported by the National Cancer Control Program funded by the Ministry of Health and Welfare in Korea (number 1220210). The publication was partially supported by the BK21 Research Fellowship from the Ministry of Education, Science and Technology, Republic of Korea. H.-Y.J. was the recipient of a Seoul Science Fellowship.

References

- 1 Glover DM, Leibowitz MH, McLean DA & Parry H (1995) Mutations in aurora prevent centrosome separation leading to the formation of monopolar spindles. *Cell* **81**, 95–105.
- 2 Andrews PD, Knatko E, Moore WJ & Swedlow JR (2003) Mitotic mechanics: the auroras come into view. *Curr Opin Cell Biol* **15**, 672–683.
- 3 Barr AR & Gergely F (2007) Aurora-A: the maker and breaker of spindle poles. *J Cell Sci* **120**, 2987–2996.
- 4 Cowley DO, Rivera-Perez JA, Schliekelman M, He YJ, Oliver TG, Lu L, O'Quinn R, Salmon ED, Magnuson T & Van Dyke T (2009) Aurora-A kinase is essential for bipolar spindle formation and early development. *Mol Cell Biol* **29**, 1059–1071.
- 5 Macurek L, Lindqvist A, Lim D, Lampson MA, Klompaker R, Freire R, Clouin C, Taylor SS, Yaffe MB & Medema RH (2008) Polo-like kinase-1 is activated by aurora A to promote checkpoint recovery. *Nature* **455**, 119–123.
- 6 Zhou H, Kuang J, Zhong L, Kuo WL, Gray JW, Sahin A, Brinkley BR & Sen S (1998) Tumour amplified kinase STK15/BTAK induces centrosome amplification, aneuploidy and transformation. *Nat Genet* **20**, 189–193.
- 7 Bischoff JR, Anderson L, Zhu Y, Mossie K, Ng L, Souza B, Schryver B, Flanagan P, Clairvoyant F, Ginther C *et al.* (1998) A homologue of *Drosophila* aurora kinase is oncogenic and amplified in human colorectal cancers. *EMBO J* **17**, 3052–3065.
- 8 Nikonova AS, Astsaturov I, Serebriiikii IG, Dunbrack RL Jr & Golemis EA (2013) Aurora A kinase (AURKA) in normal and pathological cell division. *Cell Mol Life Sci* **70**, 661–687.
- 9 Keen N & Taylor S (2004) Aurora-kinase inhibitors as anticancer agents. *Nat Rev Cancer* **4**, 927–936.
- 10 Dutertre S, Descamps S & Prigent C (2002) On the role of aurora-A in centrosome function. *Oncogene* **21**, 6175–6183.
- 11 Lu LY, Wood JL, Ye L, Minter-Dykhouse K, Saunders TL, Yu X & Chen J (2008) Aurora A is

- essential for early embryonic development and tumor suppression. *J Biol Chem* **283**, 31785–31790.
- 12 Dees EC, Infante JR, Cohen RB, O'Neil BH, Jones S, von Mehren M, Danaee H, Lee Y, Ecsedy J, Manfredi M *et al.* (2011) Phase I study of MLN8054, a selective inhibitor of Aurora A kinase in patients with advanced solid tumors. *Cancer Chemother Pharmacol* **67**, 945–954.
 - 13 Kallio MJ, McClelland ML, Stukenberg PT & Gorbisky GJ (2002) Inhibition of aurora B kinase blocks chromosome segregation, overrides the spindle checkpoint, and perturbs microtubule dynamics in mitosis. *Curr Biol* **12**, 900–905.
 - 14 Schmit TL, Zhong W, Setaluri V, Spiegelman VS & Ahmad N (2009) Targeted depletion of Polo-like kinase (Plk) 1 through lentiviral shRNA or a small-molecule inhibitor causes mitotic catastrophe and induction of apoptosis in human melanoma cells. *J Invest Dermatol* **129**, 2843–2853.
 - 15 Nasevicius A & Ekker SC (2000) Effective targeted gene 'knockdown' in zebrafish. *Nat Genet* **26**, 216–220.
 - 16 Bruce AE, Howley C, Zhou Y, Vickers SL, Silver LM, King ML & Ho RK (2003) The maternally expressed zebrafish T-box gene *comesodermin* regulates organizer formation. *Development* **130**, 5503–5517.
 - 17 Hendzel MJ, Wei Y, Mancini MA, Van Hooser A, Ranalli T, Brinkley BR, Bazett-Jones DP & Allis CD (1997) Mitosis-specific phosphorylation of histone H3 initiates primarily within pericentromeric heterochromatin during G₂ and spreads in an ordered fashion coincident with mitotic chromosome condensation. *Chromosoma* **106**, 348–360.
 - 18 Davis FM, Tsao TY, Fowler SK & Rao PN (1983) Monoclonal antibodies to mitotic cells. *Proc Natl Acad Sci USA* **80**, 2926–2930.
 - 19 Choi E, Choe H, Min J, Choi JY, Kim J & Lee H (2009) BubR1 acetylation at prometaphase is required for modulating APC/C activity and timing of mitosis. *EMBO J* **28**, 2077–2089.
 - 20 Lee H, Trainer AH, Friedman LS, Thistlethwaite FC, Evans MJ, Ponder BA & Venkitaraman AR (1999) Mitotic checkpoint inactivation fosters transformation in cells lacking the breast cancer susceptibility gene, *Brca2*. *Mol Cell* **4**, 1–10.
 - 21 Jeong K, Jeong JY, Lee HO, Choi E & Lee H (2010) Inhibition of Plk1 induces mitotic infidelity and embryonic growth defects in developing zebrafish embryos. *Dev Biol* **345**, 34–48.
 - 22 Chan GK, Liu ST & Yen TJ (2005) Kinetochore structure and function. *Trends Cell Biol* **15**, 589–598.
 - 23 Yu H (2006) Structural activation of Mad2 in the mitotic spindle checkpoint: the two-state Mad2 model versus the Mad2 template model. *J Cell Biol* **173**, 153–157.
 - 24 Huang YF, Chang MD & Shieh SY (2009) TTK/hMps1 mediates the p53-dependent postmitotic checkpoint by phosphorylating p53 at Thr18. *Mol Cell Biol* **29**, 2935–2944.
 - 25 Ganansia-Leymarie V, Bischoff P, Bergerat JP & Holl V (2003) Signal transduction pathways of taxanes-induced apoptosis. *Curr Med Chem Anticancer Agents* **3**, 291–306.
 - 26 Robu ME, Larson JD, Nasevicius A, Beiraghi S, Brenner C, Farber SA & Ekker SC (2007) p53 activation by knockdown technologies. *PLoS Genet* **3**, e78.
 - 27 Logarinho E & Bousbaa H (2008) Kinetochore-microtubule interactions 'in check' by Bub1, Bub3 and BubR1: the dual task of attaching and signalling. *Cell Cycle* **7**, 1763–1768.
 - 28 Marumoto T, Honda S, Hara T, Nitta M, Hirota T, Kohmura E & Saya H (2003) Aurora-A kinase maintains the fidelity of early and late mitotic events in HeLa cells. *J Biol Chem* **278**, 51786–51795.
 - 29 Budirahardja Y & Gonczy P (2009) Coupling the cell cycle to development. *Development* **136**, 2861–2872.
 - 30 Langenau DM, Traver D, Ferrando AA, Kutok JL, Aster JC, Kanki JP, Lin S, Prochownik E, Trede NS, Zon LI *et al.* (2003) Myc-induced T cell leukemia in transgenic zebrafish. *Science* **299**, 887–890.
 - 31 Santoriello C & Zon LI (2012) Hooked! Modeling human disease in zebrafish. *J Clin Invest* **122**, 2337–2343.
 - 32 Feitsma H & Cuppen E (2008) Zebrafish as a cancer model. *Mol Cancer Res* **6**, 685–694.
 - 33 Zon LI & Peterson RT (2005) *In vivo* drug discovery in the zebrafish. *Nat Rev Drug Discov* **4**, 35–44.
 - 34 Murphey RD & Zon LI (2006) Small molecule screening in the zebrafish. *Methods* **39**, 255–261.
 - 35 Kimmel CB, Ballard WW, Kimmel SR, Ullmann B & Schilling TF (1995) Stages of embryonic development of the zebrafish. *Dev Dyn* **203**, 253–310.
 - 36 Oxtoby E & Jowett T (1993) Cloning of the zebrafish *krox-20* gene (*krx-20*) and its expression during hindbrain development. *Nucleic Acids Res* **21**, 1087–1095.

Supporting information

Additional supporting information may be found in the online version of this article at the publisher's web site:

Fig. S1. Problems in centrosome intactness, such as centrosome maturation, of Aurora-A morphants.

Fig. S2. Results for the three independent experiments summarized in Fig. 5C.

Movies S1–S4. Time-lapse video microscopy for Figure 4A–D. Movie S1, Live-imaging of Figure 4A; Movie S2, Figure 4B; Movie S3, Figure 4C; Movie S4, Figure 4D.